Journal of
Manufacturing and Materials Processing

MDPI

Article

Improved Mechanical Performance of Carbon–Kevlar Hybrid Composites with TiO_2 Nanoparticle Reinforcement for Structural Applications

Vignesh Nagarajan Jawahar [1], Rajesh Jesudoss Hynes Navasingh [2,3,*], Krzysztof Stebel [4], Radosław Jasiński [5] and Adam Niesłony [6]

[1] Department of Mechanical Engineering, SRM Madurai College for Engineering and Technology, Pottapalayam, Madurai 630612, India; vigneshsrikrishna@gmail.com
[2] Faculty of Mechanical Engineering, Opole University of Technology, Proszkowska 76, 45-758 Opole, Poland
[3] Department of Mechanical Engineering, Mepco Schlenk Engineering College, Sivakasi 626005, India
[4] Department of Automatic Control and Robotics, Faculty of Automatic Control, Electronics and Computer Science, Silesian University of Technology, 44-100 Gliwice, Poland; krzysztof.stebel@polsl.pl
[5] Department of Building Structures and Laboratory of Civil Engineering Faculty, Faculty of Civil Engineering, Silesian University of Technology, Akademicka 5, 44-100 Gliwice, Poland; radoslaw.jasinski@polsl.pl
[6] Department of Mechanics and Machine Design, Faculty of Mechanical Engineering, Opole University of Technology, 45-758 Opole, Poland; a.nieslony@po.edu.pl
* Correspondence: findhynes@yahoo.co.in

Abstract: Carbon–Kevlar hybrid composites are being increasingly recognized as suitable materials for aerospace, automotive, and construction applications due to their unique combination of strength, toughness, and safety. Prior to their use, extensive testing and validation are essential to ensure that these composites meet the specific safety and performance standards required by each industry. In this study, the mechanical performance and behavior of five different types of Carbon–Kevlar hybrid composites were investigated. In addition to microstructural investigations, mechanical tests were also carried out, including tensile, bending, impact, and micro-hardness tests. The investigated composites were Carbon–Kevlar hybrids without orientation, with a symmetrical orientation, and with the addition of TiO_2 nanoparticles at weight percentages of 3%, 4%, and 5%. The results showed that the mechanical properties of these composites could be significantly influenced by different fiber orientations and the addition of TiO_2 nanoparticles. In particular, the addition of TiO_2 nanoparticles increased the tensile strength, hardness, toughness, and breaking strength. Of the composites tested, the composite reinforced with 5% TiO_2 nanoparticles exhibited the highest mechanical performance, with a 79.8 Shore D hardness, 406 MPa tensile strength, 398 N/mm^2 flexural strength, and 10.1 J impact energy. These results indicate that Carbon–Kevlar hybrid composites reinforced with TiO_2 nanoparticles have excellent mechanical properties that make them highly suitable for armor plating, helmets, and vehicle armoring in particular and a wide range of other industrial applications in general.

Keywords: hybrid composites; carbon fibers; Kevlar fibers; fiber orientation; TiO_2 nanoparticles; mechanical performance; flexural strength; microstructural investigation

check for updates

Academic Editor: Shuting Lei

Received: 31 March 2025
Revised: 18 April 2025
Accepted: 19 April 2025
Published: 24 April 2025

Citation: Jawahar, V.N.; Navasingh, R.J.H.; Stebel, K.; Jasiński, R.; Niesłony, A. Improved Mechanical Performance of Carbon–Kevlar Hybrid Composites with TiO_2 Nanoparticle Reinforcement for Structural Applications. *J. Manuf. Mater. Process.* **2025**, *9*, 140. https://doi.org/10.3390/jmmp9050140

Copyright: © 2025 by the authors. Licensee MDPI, Basel, Switzerland. This article is an open access article distributed under the terms and conditions of the Creative Commons Attribution (CC BY) license (https://creativecommons.org/licenses/by/4.0/).

1. Introduction

The lower interlaminar fracture toughness of Carbon fiber-reinforced composites makes them favorable for use in several fields such as military, automotive, and aerospace

applications. Recently, the use of polymer matrix composites has been increased by many folds, as incorporating high-strength fibers into a brittle matrix enables a superior quality for aerospace and automobile components. On the other hand, when comparing the expenses and manufacturing prices with those of metals such as aluminum and steel, fiber-reinforced polymer composites are very cost-effective. They also permit the improvement of other properties such as resistance to fatigue loads and a higher specific toughness and strength. Hence, there is a need for the use of these composites in various fields, predominantly in the sports, automotive, aerospace, and construction industries [1]. Further, fiber-reinforced composites have found applications in other areas such as the fuselage skin of airplanes, helicopters, panels of truck cabs and cars, sports shoes, tennis rackets, fishing rods, and golf club shafts [2,3]. The interlocking pattern of woven fibers such as weft yarns, warp yarns, and bundles triggers a higher resistance to crack growth. Additionally, they exhibit a higher strain-to-failure ratio during compression, tension, and impact. For achieving a higher composite performance, epoxy resin is used more commonly as a matrix or binding material due to its very good stability in dimension, chemical resistance, and higher stiffness [4–6], with Carbon, Kevlar, and glass fibers as reinforcements [7].

It was reported by Pathak et al. [8] that fillers like graphene oxide can be used for the reinforcement step in the process of developing Carbon fiber/graphene oxide–epoxy hybrid composites to improve the mechanical behavior of polymer composites. The core component of such hydrogen-bonded composites with graphene oxide not only prevents the Carbon fibers from breaking apart, but also forms hydrogen bonds with Carbon fibers to further enhance the tensile strength and modulus. This can be corroborated by the mechanical interlocking of the filler materials between the Carbon fiber and epoxy resin. Ogasawara et al. [9] reported that by adding fullerene (0.1–1 wt. %) into the matrix resin, the interlaminar fracture toughness could be increased by 60%. Vaganoy et al. [10], in their work, reported that by adding 1.0% by wt. of CNTs to Carbon fiber-reinforced epoxy composites, it was possible to increase the fracture toughness by about 40%. Xu et al. [11] reported that when clay is added as an additive material to Carbon fiber/epoxy composites, an enhancement in the flexural properties may occur.

McGrath et al. [12] investigated the influence of alumina powder on the mechanical properties of epoxy composites. Their study reported that by varying parameters such as particle size distribution, size, and shape, only a small effect on the final mechanical properties could be obtained [13]. But the most critical factors enabling changes in such properties are the resin cross-link density and filler loading. Kardar et al. [14] investigated the physical–mechanical properties of UV-cured epoxy acrylate manufactured with different nano alumina particles by applying nanoindentation. Their study revealed that the existence of nanoparticles helped to enhance the self-healing and scratch resistance capability of the film. The water absorption effect on the nano-alumina-filled epoxy nanocomposites was investigated and the mechanical and dielectric properties were studied [15,16]. Their study showed that, due to the addition of nano alumina to the composites, there was an increase in stiffness. Furthermore, the interfacial area increased the dielectric properties. Zhao et al. [17] performed research on the mechanical characteristics of nano-filled epoxy with alumina nanoparticles. The authors noted that an improved tensile strength of the composites corresponded to stronger interfacial bonding. The primary mechanisms of failure were crack deflection and microcracking.

Mirmohseni and Zavareh [18] used nano TiO_2 as a filler material to study its influence on improvements in the toughness of composites. Their study found that nanofillers improve the tensile and impact strength when compared to pure composites. Chatterjee and Islam [19] investigated the influence of TiO_2 nanofillers on the mechanical properties of epoxy nanocomposites. Properties such as viscoelastic, thermal, and mechanical were

improved by the addition of nanofillers. They further noted that there was an increase in the tensile modulus Tg, flexural modulus, short beam strength, and storage modulus when compared to normal epoxy composites without any nanofillers. Zhou et al. [20] carried out a study on the flexural and failure modes of fiber-reinforced epoxy composites when TiO_2 particles were added as additives. The size and weight fraction of the particles were varied, and their effects were studied. They found that increasing the addition of TiO_2 by more than 1% was associated with a reduction in the mechanical properties. This is because a higher stress concentration can occur by the agglomeration of nanoparticles. Hamming et al. [21] studied the macro-scale properties of TiO_2 polymer matrix composites in terms of the interfacial modification effect and the dispersion of the nanoparticles. They found a decrease in the Tg when an increase in the wt. % of the unmodified nanoparticles happened. Tg is highly sensitive to the quality of the dispersion of nanoparticles and the quality of interfacial interaction. Siddhartha et al. [22], in their study, reported that there was an increase in flexural strength, tensile strength, tensile modulus, and impact strength when fillers were added to composites by up to 20%. Rajesh et al. [23], in their work, carried out the fabrication of GFRPs with different proportions of aluminum oxide and silicon carbide using epoxy and polyester resins. The final result was better when compared to composites fabricated by polyester resin. Naik et al. [24] studied the performance of composite laminae with only Carbon and only glass reinforcements. They found that the notch sensitivity for hybrid composites was lower compared to the above two types of reinforcements.

Hence, in the literature, it can be seen that the mechanical properties of composites improve significantly with the addition of filler materials such as nanoparticles. Carbon fibers possess a high tensile strength and stiffness, while Kevlar fibers offer an excellent impact resistance, toughness, and thermal stability. By combining these fibers in a hybrid composite, the overall mechanical performance can be improved, making trade-offs between the advantages of each material to match the needs of specific structural applications. One of the major drawbacks of Carbon–Kevlar composites is that they are more expensive than metals. They can also exhibit a poor inter laminar fracture toughness, i.e., not performing as well under some loading conditions like shear. Enhancement of this can be achieved through the incorporation of TiO_2 nanoparticles as reinforcements into these composite structures, which results in improved mechanical characteristics such as an increased tensile strength, hardness, toughness, and impact strength. Nanoparticles serve as fillers that improve matrix–fiber bonding, resulting in an overall improved performance with a better strength and durability. A study on the mechanical performance of Carbon–Kevlar fiber-reinforced epoxy composites manufactured with TiO_2 nanoparticles by varying the wt. % has not been carried out so far. Hence, this paper deals with the study of the mechanical performance and microstructural properties of Carbon–Kevlar hybrid epoxy composites with TiO_2 reinforcements. Control samples were used without nano additives (with and without orientation). The present work distinguishes itself from others by combining both the orientation of fibers and the addition of TiO_2 nanoparticles in a hybrid composite system.

2. Materials and Methods

The materials used to develop the composites included Carbon Fiber 600 gsm, Kevlar Fiber 49, Titanium Oxide nanoparticles (TiO_2), Epoxy Resin Araldite LY 556, and Hardener Aradur HY 951. The nanoparticles and all other required raw materials were obtained from a retailer named SM Composites, Chennai. Titanium Oxide nanoparticles were purchased from Platonic Nanotech Private Limited, Jharkhand, India. The Titanium Oxide nanoparticles used had an average particle size of 30–50 nm and a specific surface area of 200–230 m^2/g. They had a bulk density of 0.15–0.25 g/cm^3 and a true density of 4.23 g/cm^3.

The morphology of the nanoparticles was spherical. The purity of the nanopowder was about 99.99% and the color was white. The chemical proportion of the TiO_2 nanoparticles is shown in Table 1.

Table 1. Chemical composition of TiO_2 nanoparticles.

Material	TiO_2	S	Si	Mg	Al
% Composition	>99.9	<0.05	<0.02	<0.01	<0.01

2.1. Development of Carbon–Kevlar Hybrid Composites

The Carbon–Kevlar hybrid composites were developed using the compression molding technique. To create an effective composite with a superior performance, the material should be selected from various compositions. Here, to find the best one, we chose 5 different configurations, and for simplification, they are abbreviated as follows: (i) Carbon–Kevlar hybrid composites without any orientation as (Type I), (ii) Carbon–Kevlar hybrid composites with a symmetric orientation as C(+45°)K(−45°)C(90°)K(0°)C(90°)K(−45°)C(+45°) as (Type II), (iii) Carbon–Kevlar hybrid composites with 10 gm Titanium Oxide nano reinforcements as (Type III), (iv) Carbon–Kevlar hybrid composites with 12.5 gm Titanium Oxide nano reinforcements as (Type IV), and (v) Carbon–Kevlar hybrid composites with 15 gm Titanium Oxide nano reinforcements as (Type V).

The size of the die used was 150 mm × 250 mm × 5 mm. Initially, the purchased Carbon and Kevlar fibers were cut as per the dimensions of the die, which had a length of 250 mm and breadth of 150 mm. A total of 7 layers of fibers were stacked alternatively as Carbon fibers (4 Nos) and Kevlar fibers (3 Nos). Hence, the sequence was abbreviated as CKCKCKC, with details presented in Figure 1. The same type of sequencing arrangement was followed in all the developed cases studied here.

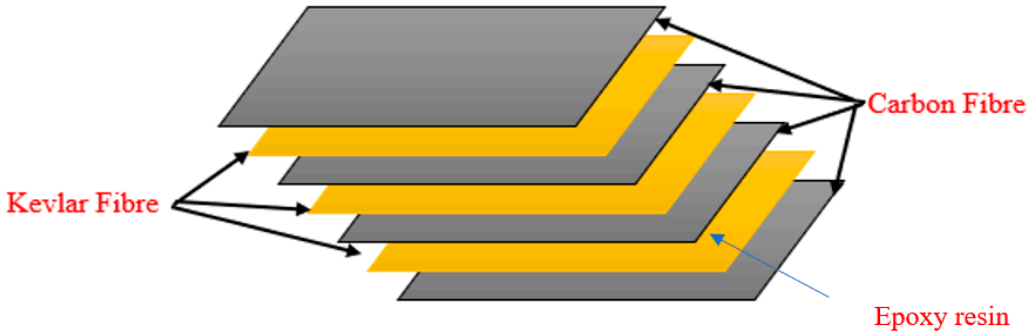


Figure 1. Stacking sequence of Carbon–Kevlar hybrid composites.

Epoxy resin and hardener were mixed in the desired ratio as per the rule of mixture, which is assumed to find the suitable mass fraction of resin and mass fraction of fibers, respectively. The composites were allowed to settle for a while between 8 h and 24 h in a compression molding machine. The compression molding machine was purchased available in the Department of Mechanical Engineering, Mepco Schlenk Engineering College, Sivakasi, Tamil Nadu, India. It is purchased from JRD Rubber and Plastic Technology Pvt. Ltd., New Delhi, India. The machine has a capacity of 60 tones and it is a downward compression molding machine. After the settling time, the composite was removed from the mold. The final composite structure is shown in Figure 2. This figure shows the composite structure that was developed without any orientation (Type I). Then, Carbon–Kevlar hybrid composites with a symmetric orientation were developed as C(+45°)K(−45°)C(90°)K(0°)C(90°)K(−45°)C(+45°). Here, the size of the fibers was sim-

ilar as that in the previous case, and the mass fraction was also the same for the fibers and matrix.



Figure 2. Carbon–Kevlar hybrid composite without any orientation.

The preparation of nano-reinforced Carbon–Kevlar hybrid composites was performed with three percentage compositions using TiO_2 nanoparticles as reinforcements. The percentage compositions were 3%, 4%, and 5% by weight, respectively. The nanoparticles were initially weighed using a standard weighing machine and then mixed with the epoxy resin, as shown in Figure 3.

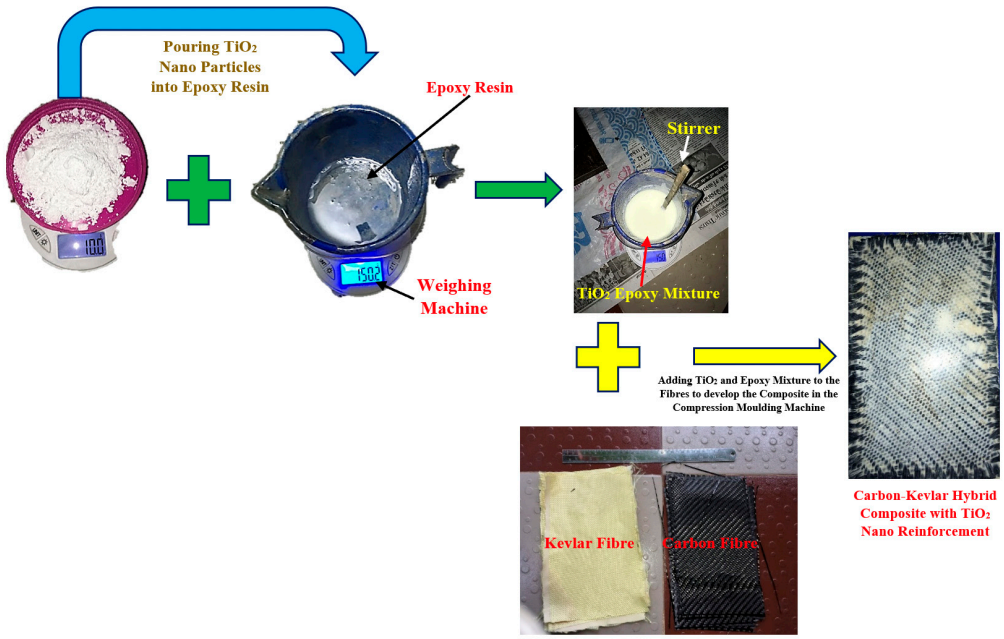


Figure 3. Preparation of nano-reinforced Carbon–Kevlar hybrid composites.

A conventional direct mixing technique was used for mixing the nanoparticles with the epoxy resin. The mixing process was carried out for 5 min to allow for uniform mixing. After

preparing the nano–resin mixture, the novel composite was manufactured as described in the procedures for preparing the Carbon–Kevlar hybrid composites. Initially, the die was filled with the mixture and a standard paintbrush and squeezer were used to completely spread out the resin mixture on the base of the die. Then the first layer of Carbon fiber was laid on it. Further, once again, the resin was poured and spread out on the top of the first layer of Carbon fiber. Here, the squeezer was used to evenly spread out the resin mixture in all areas. Then, the Kevlar fiber was laid on top, which was followed by a coating of resin. In this way, the layup was conducted up to 7 layers, and then using the squeezer, the excess resin was removed to prevent the formation of any void content in the composite. After this, the male die was placed over the female die and the entire setup was kept inside the compression molding machine for 8 h. Finally, after the settled time, the composite was taken from the die. Figure 4 shows a pictorial view of the manufactured Carbon–Kevlar hybrid composite containing TiO_2 nano reinforcements. Details of three weight percentages of 3%, 4%, and 5%, respectively, are presented.



(**a**) (**b**) (**c**)

Figure 4. (**a**) Carbon–Kevlar hybrid composites with TiO_2 nano reinforcements 3%, (**b**) 4%, and (**c**) 5% by weight sample, respectively.

2.2. Performance Evaluation

To evaluate the performance of the composites developed, they were subjected to various mechanical tests. Before carrying out the tests, the samples were prepared as per the ASTM standards D638 [25], D 790 [26] & D 256 [27] for Tensile, Flexural and Impact testing respectively. The outcomes of these tests were used to identify the best candidate sample for aerospace applications. The following tests were carried out to check their performance.

2.2.1. Tensile Test

A tensile test was carried out to find out the value of the maximum pulling force that the prepared samples could withstand before failure took place. The tensile tests were carried out according to the ASTM D638 standard. The dimensions used for preparing the samples are given in Figure 5g as per ASTM D638 standards. Details of the configuration of the samples prepared are shown in Figure 5. To carry out the tensile test, three samples from each composite material were cut from the center of the material. The test was carried out under a UTM Machine, manufactured by Associated Scientific Engg. Works, New Delhi. The maximum load capacity of this machine was 50 kN (5 Ton, class 0.5).

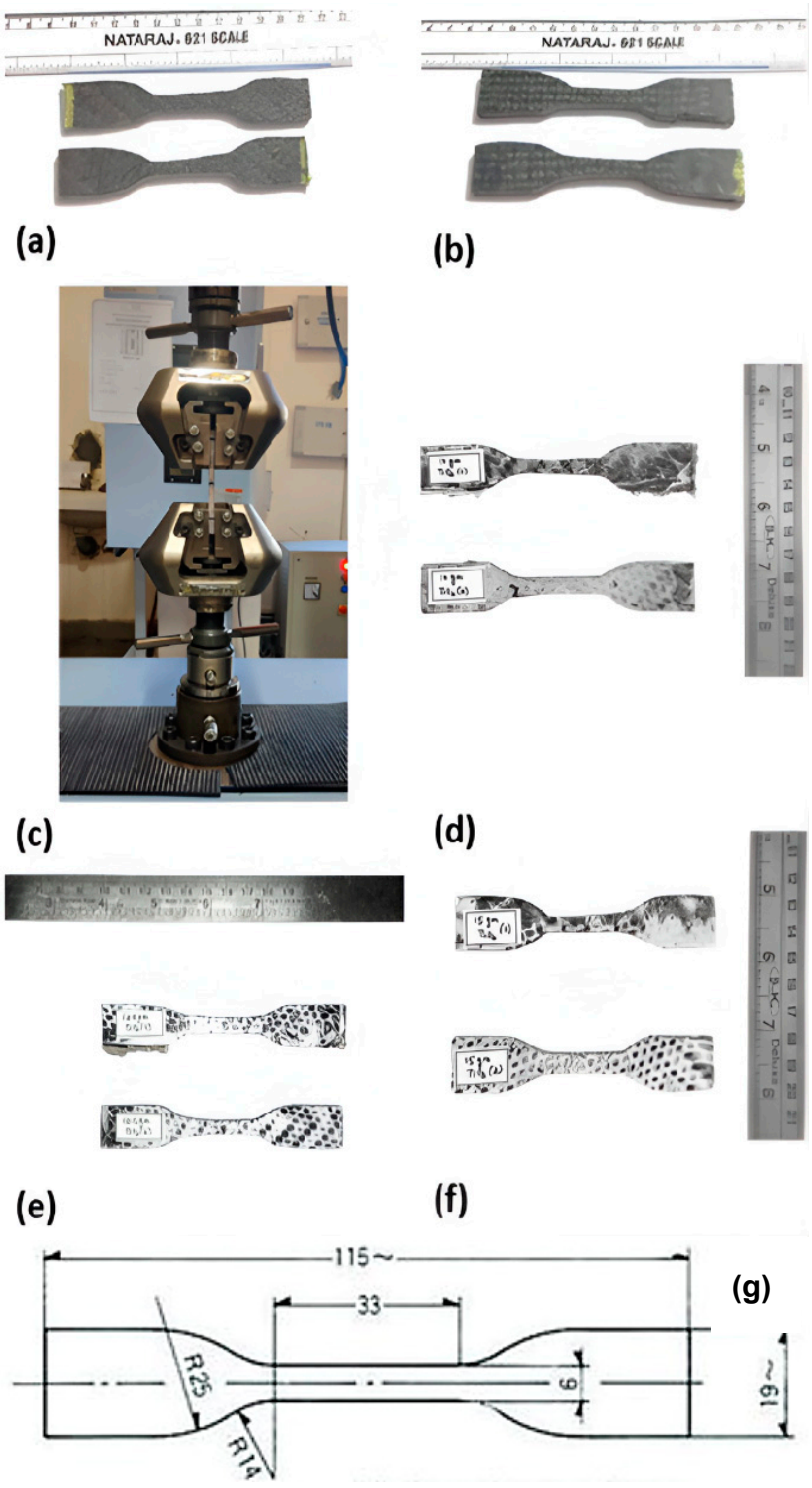


Figure 5. Tensile test samples prepared as per ASTM D638 standards for: (**a**) Type I, (**b**) Type II, (**c**) specimen placed in the testing machine, (**d**) Type III, (**e**) Type IV, (**f**) Type V, and (**g**) ASTM D638 standard.

2.2.2. Flexural Test

To find out the sample modulus of rupture, flexural tests were carried out. This is a test which permits one to find out the amount of force that is needed to bend a beam under a 3-point load. This test can evaluate the stiffness of a material. This test was carried out under ambient conditions of temperature and pressure. Figure 6 shows the various samples that were used for carrying out the flexural tests. The standard dimensions used to carry out the evaluation were according to ASTM D 790. The dimensions used for preparing the

samples are given in Figure 6g as per ASTM D 790 standards. The testing was conducted on three-point bending test equipment manufactured by Shimadzu Corporation, Kyoto, Japan.

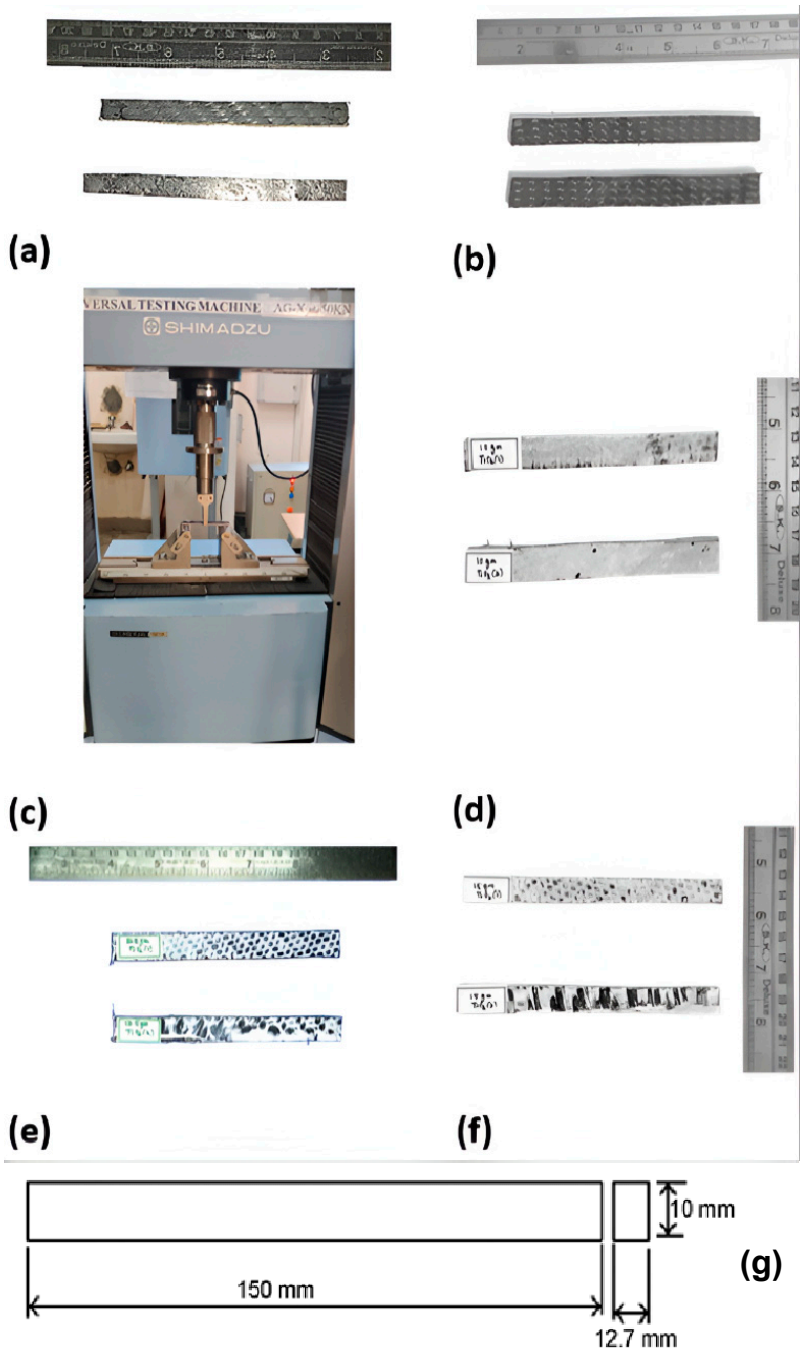


Figure 6. Flexural testing as per ASTMD 790 standards: (**a**) Type I, (**b**) Type II, (**c**) specimen placed in the testing machine, (**d**) Type III, (**e**) Type IV, (**f**) Type V, and (**g**) ASTM D 790 standard.

2.2.3. Impact Test

The composites manufactured were subjected to impact tests. These tests allowed us to find out the toughness of the material manufactured. The amount of energy that is absorbed by a material during plastic deformation is said to be called material toughness. When compared with ductile materials, brittle materials have a lower value of toughness. This is because they can withstand only the minimum value of plastic deformation. When a material is tested under temperature, a change in the toughness occurs. For example, when the testing temperature is very low, the impact resistance of the material tested is low too.

By varying the size of the sample, some changes in the sample impact value can also occur. This is because, in some cases, the imperfections in these samples may increase, which acts as a stress riser. Figure 7 shows the various samples used to detect impact characteristics. The standard used to evaluate the impact resistance was ASTM D 256. The dimensions used for preparing the samples are given in Figure 6g, as per ASTM D 256 standards. This test was carried out on an Izod impact tester manufactured by AIT Testing Equipment Co., Ltd., Dongguan, Guangdong, China.

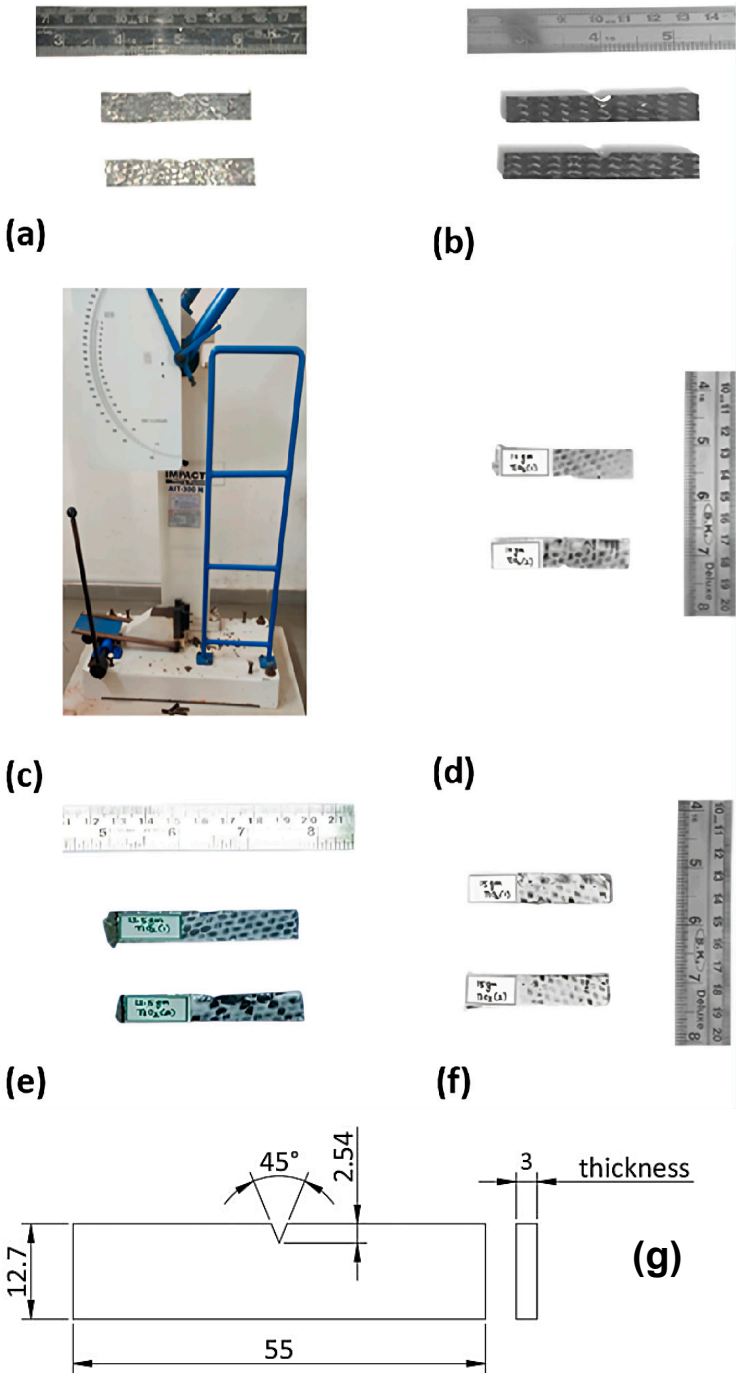


Figure 7. Details of impact testing samples prepared as per ASTM D 256 standards for: (**a**) Type I, (**b**) Type II, (**c**) specimen placed in the impact testing apparatus, (**d**) Type III, (**e**) Type IV, (**f**) Type V machine, and (**g**) ASTM D 256 standard.

2.2.4. Hardness Test

To find out the hardness of the manufactured sample product, a Shore D test was performed on it. To measure the Shore hardness, we used an instrument called a Durometer. The Durometer intender foot is made to penetrate samples to detect their hardness. The samples were cut into 20 mm × 20 mm and they were ground to a smooth flatness using a grinding machine before carrying out the hardness test. The details of samples prepared to evaluate the hardness resistance are shown in Figure 8. The tester used to carry out the Shore D hardness test was manufactured by Mitutoyo.

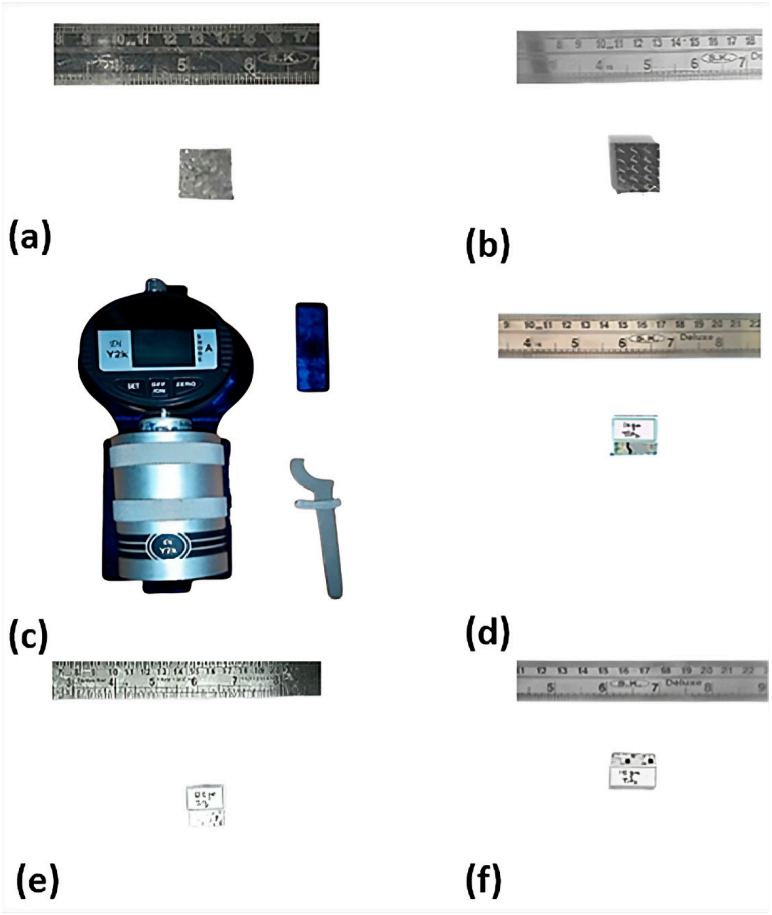


Figure 8. Shore D hardness testing sample prepared as per ASTM standards for: (**a**) Type I, (**b**) Type II, (**c**) Shore D hardness testing machine, (**d**) Type III, (**e**) Type IV, and (**f**) Type V.

2.2.5. Microstructural Investigation and Fractography

Microstructural investigation is a very powerful technique to find out the structural morphology of a composite structure. It also permitted us to find out the various layer structures in the manufactured composite, their bonding nature, fiber orientation, and the size of the particles. The microstructure was taken from the Scanning Electron Microscope (EVO18 (CARL ZEISS)) facility available at Kalasalingam University, Krishnankoil, Virudhunagar District, Tamil Nadu. The samples were prepared accordingly, and they were bounded by a cross-section of 10 mm × 10 mm. In addition, SEM was used to carry out the fractography of the tested samples to detect fiber damage, pull out, and other imperfections that formed during the manufacturing of the composite.

3. Results and Discussions

Figure 9 shows the samples after the tensile test. This permits us to see the point where the fracture takes place. Since composites act as a brittle material, the point of failure does not take place exactly at the center of the sample in all cases. Further, there is no formation of any necking region and, hence, it is a pure brittle failure. Failure takes place at different points in all five different samples. After evaluating the results of the tensile tests, we can notice a steady increase in the ultimate tensile strength for the samples evaluated, as shown in Figure 10. The Carbon fiber has a very good tensile strength, however, it is very brittle, with a good rigidity and a higher strength to weight ratio. On the other hand, the Kevlar fiber has a very good impact resistance, toughness, and thermal stability. Hence, by combining these two compounds, it is possible to improve the properties of novel materials. In addition to this, the addition of titanium oxide nanoparticles helps to increase the strength of the composite structure greatly.

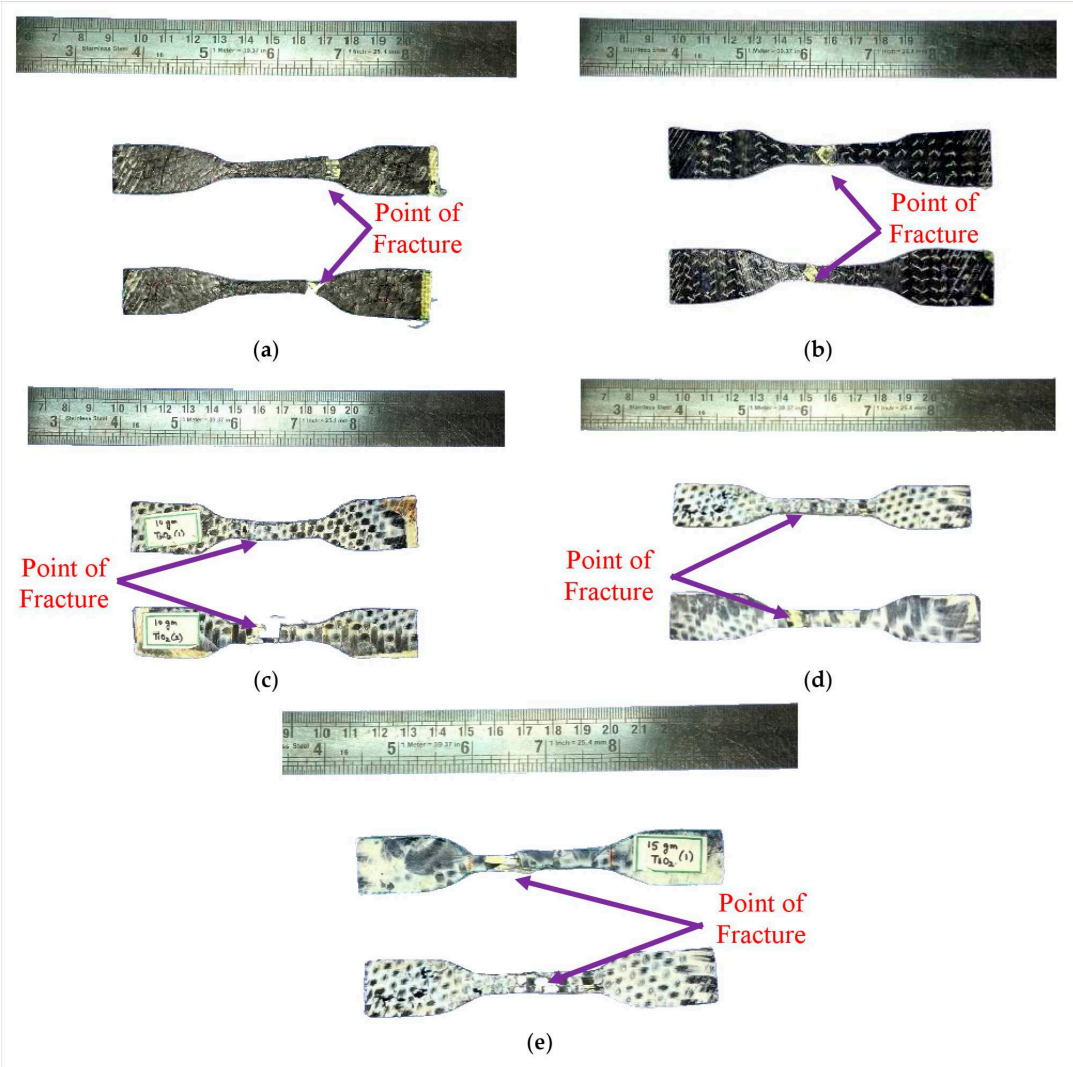


Figure 9. The sample shape after conducting the tensile test for: (**a**) Type I, (**b**) Type II, (**c**) Type III, (**d**) Type IV, and (**e**) Type V.

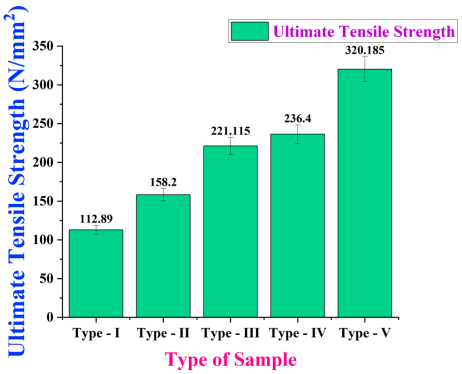


Figure 10. Ultimate tensile strength for 5 different types of samples studied.

Table 2 shows the tensile test results that were obtained for the various samples. For each type, three samples were prepared for conducting the tensile tests, and the average value of the tests is displayed. From Table 2, it can be seen that the increase in the tensile strength was produced at the expense of the reduction in percentage elongation. This was also observed by Hamidon et al. [28]. However, not all cases followed the same pattern. Further, the decrease in the percentage elongation was not directly proportional with strength, as seen in Table 2. At the same time, whenever a material has a higher tensile strength, it does not mean that the material is a good one, and vice versa. It depends on where the material is used [28].

Table 2. Tensile test output.

S. No.	Sample:	Tensile Strength (N/mm^2)	Maximum Strain	Elongation (%)	Tensile Load (kN)	Maximum Displacement (mm)
1	Type I	113	18.3	17.4	4.81	6.57
2	Type II	158	26.3	21.3	5.39	9.47
3	Type III	221	22.6	9.50	7.36	8.14
4	Type IV	236	36.3	26.7	10.1	10.9
5	Type V	320	31.9	16.6	10.6	11.5
		Standard Deviation	79.07	7.18	6.34	2.64

The results demonstrate that the introduction of nano additives should improve the tensile strength of the composites manufactured. Out of the two fibers used, Carbon fibers help to enhance the strength of the final composites made and Kevlar fibers aid in improving the stiffness of the composites. Moreover, the strength increases further with the addition of TiO_2 nanoparticles. An increase of 15% in the weight of the TiO_2 nanoparticles improves the tensile strength of the developed composites (Type V) to about 184% when compared to the composite without any nanoparticle addition (Type I) [29].

Figure 10 shows the ultimate tensile strength plot for different types (Type I to Type V) of samples. From the graph, it can be seen that there is a steady increase in the ultimate tensile strengths of different types of samples. The value of the maximum tensile strength is about 320 N/mm^2 for Type V and the minimum value is around 113 N/mm^2 for Type I. This proves that the strength of the composites increases during the change in the orientation of the composite fibers used, and also during the addition of nano-reinforcements. When we check Type I against the rest of the sample types (i.e., from Type II to Type V), we can see that there is an increase of about 40% in the ultimate tensile strength for Type II samples, 96% for Type III, 109% for Type IV, and 184% for Type V, respectively. Hence, adding nano reinforcements into the composites enables improving the strength, which is about three times greater than ordinary hybrid composites and two times greater than fiber-oriented

hybrid composites. Further, the load capacity for all sample types is noted to increase up to a maximum of 10.6 kN for Type V, while the lowest is 4.81 kN for Type I. Therefore, the nanoparticles permit an increase of up to ten times the withstanding load before failure takes place. In other words, the composites with a symmetric fiber orientation are stiffer than those without orientation, and the composites with nanoparticle reinforcement are further stiffer than the rest.

Figure 11 shows the stress vs strain curve for all five different types of samples. Here, we can observe that, for Type I and Type II, the maximum stress values obtained are about 177 N/mm^2 and 204 N/mm^2, respectively. However, when adding TiO_2 nanoparticles to the hybrid composites, the maximum values of stress obtained are 325 N/mm^2, 348 N/mm^2, and 406 N/mm^2 for Type III, Type IV, and Type V, respectively. The percentage differences in the improvement of the maximum stress value obtained by comparing the composites without orientation (Type I) to those with nanoparticle addition are about 83%, 96%, and 129% for Type III, Type IV, and Type V, respectively. In the same way, comparing the maximum stress value of Type II with nanoparticle addition, the percentage differences are about 59%, 70%, and 99% for Type III, Type IV, and Type V, respectively. Hence, the addition of TiO_2 nanoparticles shows a significant improvement in the stress resistance capacity of the composites.

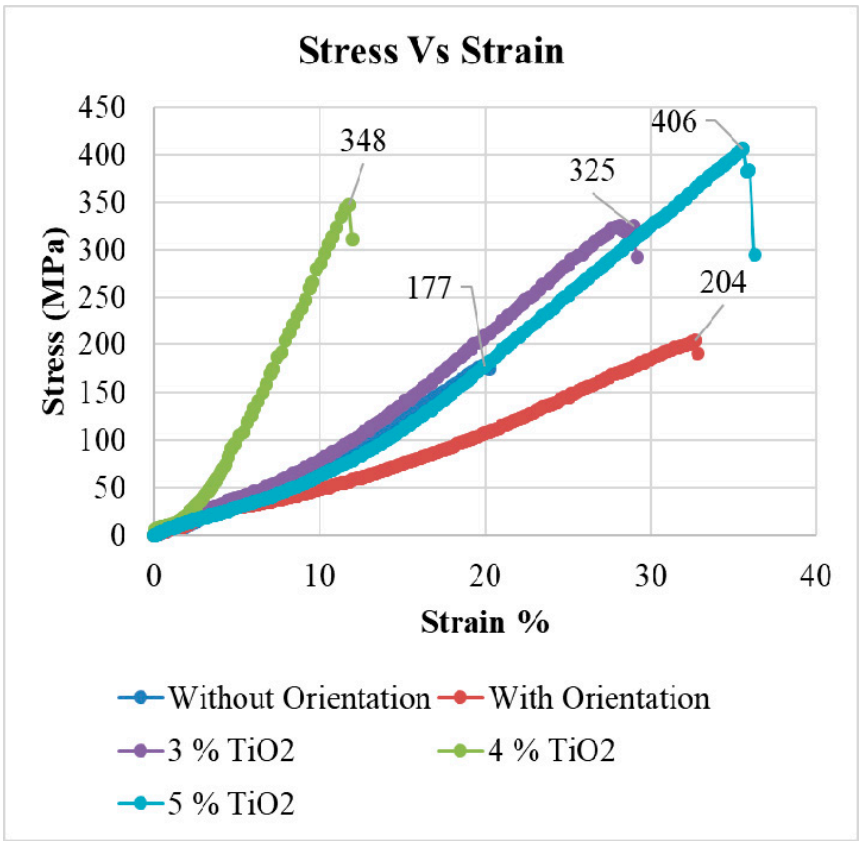


Figure 11. Stress vs. strain curve for 5 different types of samples.

From Figure 11, we can see that all the curves exhibit more or less the same pattern. All these curves prove that they are brittle, since there are no yield points in them. Once the maximum tensile stress is achieved, immediately, the failure of the samples takes place. The failure of the samples is characterized by a ticking sound, which is heard when the experiment has been carried out. During the loading process, the load is initially supported by the matrix and progressively transmitted to the reinforcements. When the matrix can no longer withstand the load, plastic deformation takes place. Then, the load is absorbed by

the fibers together. Since the material manufactured is a hybrid polymer composite, the two fibers used have various moduli of elasticity. Further, since Kevlar fibers possesses a lower elasticity as compared to their counterpart Carbon fibers, Kevlar fibers break faster than Carbon fibers. The overall elongation of Carbon fibers is somewhat longer than that of Kevlar fibers because of the higher elasticity value. This helps to extend the time before the failure of the entire sample during tensile activity. Because of this variation in moduli of elasticity, interplanar shear (slip planes) may occur in between the sheets of the fibers. The percentage of void contents, fiber uniformity, matrix distribution, and uniform distribution of nanoparticles, together, determine the tensile strength of the composites. Poor bonding and an insufficient interlaminar strength will also lead to premature failure of the composites.

The mechanism of tensile failure is described in Figure 12. When a load is applied, there is an increase in the length of the composite and, at the same time, there is a reduction in the width of the composites. Finally, failure takes place. It can be seen that the red-colored dots that fill the interstitial sites of the fiber sheets help to reduce the content of voids in the entire sample if the fabrication is performed properly. Nanoparticle distribution is an important parameter that drives the final mechanical properties of the composites developed. As shown in these figures, if the nanoparticles are distributed uniformly, this leads to an improvement in the tensile strength. On the other hand, if some agglomeration occurs in the nanoparticle distribution, then the microstructure of the material may vary across the sample and the strength value may be lower. This process is well established, providing the minimum chance for the formation of agglomerated TiO_2 nanoparticles. It is speculated that these nanoparticles will also tend to expand in dimension, as shown in the last figure. Hence, this process reveals that the addition of these nanoparticles proves to be beneficial for improvement in the strength of the composites.

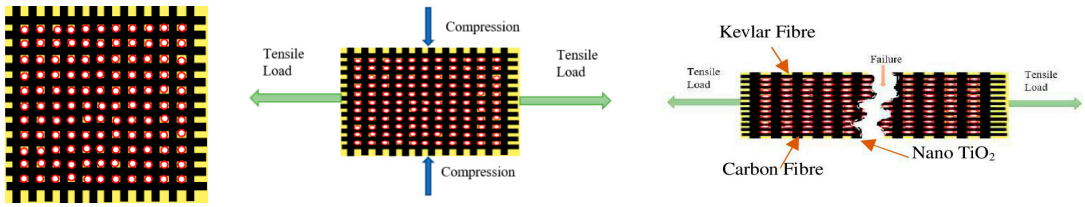


Figure 12. Mechanism of composite subjected to tensile failure.

Figure 13 shows the five different types of samples after the flexural test. The figures reveal that failure occurs at the center of the sample. Only a limited amount of fiber debonding is observed. During loading, the shear deformation starts on the laminate and failure takes place where the fiber is weaker.

Table 3 indicates the details of the flexural properties of all five types of composites manufactured. For each type of composite, three samples were tested, and their average values are given. To numerically evaluate the value of flexural stress, the following formula was used:

$$F = \frac{3xy}{2lm^2}, \text{ N/mm}^2 \quad (1)$$

where x indicates the maximum load in N, y indicates the entire span of the flexural sample in mm, l indicates the breadth of the sample in mm, and m indicates the depth of the sample in mm.

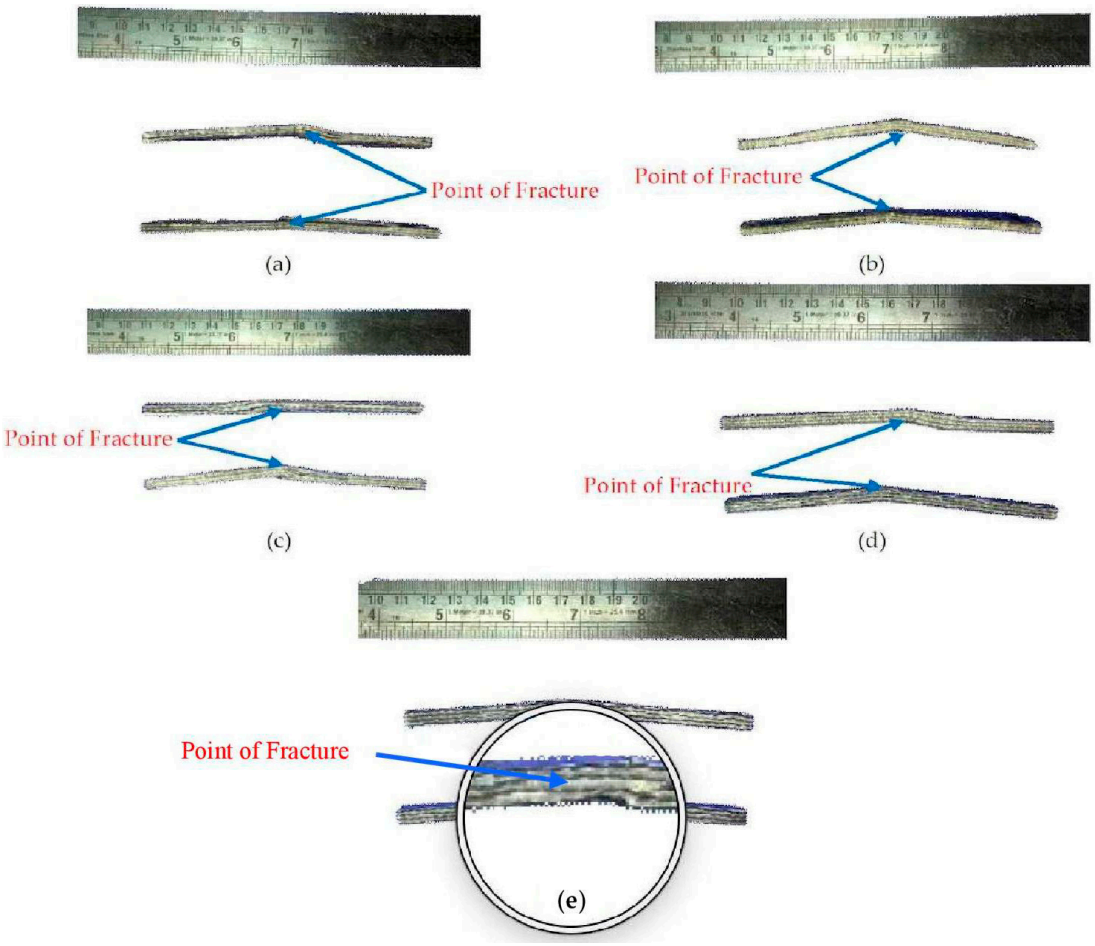


Figure 13. Details of samples after the flexural test for: (**a**) Type I, (**b**) Type II, (**c**) Type III, (**d**) Type IV, and (**e**) Type V.

Table 3. Flexural test results for the samples.

S. No.	Sample Type	Flexural Load (N)	Flexural Stress (N/mm^2)	Maximum Displacement (mm)	Stiffness (N/mm)
1	Type I	555	266	3.8	146
2	Type II	585	281	4.3	136
3	Type III	650	312	2.3	283
4	Type IV	725	348	1.9	382
5	Type V	830	398	5.9	141
Standard Deviation		111.21	53.30	1.61	110.63

A graphical view with details of the flexural load and flexural strength is shown in Figure 14a,b. The maximum value of ultimate breaking load is achieved for Type V, which is about 830 N, whereas the minimum breaking load is detected for Type I, which is 555 N. The deviation percentage between these two types of samples is about 49.5%.

Figure 14b reveals that the flexural stress is lower for the Type I sample, which shows only 266 N/mm^2, while the highest is associated with Type V, with a value of 398 N/mm^2. The rest of the samples have values between these two extremes. The percentage of increase between the maximum and minimum values of flexural stress is 49.5%. During the application of the load, the received curve is initially linear up to the maximum load and then a sudden fall occurs which follows a zig-zag pattern. This is associated with fiber breaking and the delamination of lamina during loading. 'Pinging' sounds were recorded, which is in line with Akash Deep et al.'s report [27]. Tianyu Yu et al. [30] reported that

the value of flexural strength can be improved by increasing the number of Carbon fiber layers in the composite structure and also due to the interlaminar shear strength of Carbon fiber polymers. Further, the addition of TiO_2 nanoparticles allows for further increasing the flexural strength. Nano addition leads to matrix strengthening, which can trigger the crack bridging phenomenon. Since the stiffness of TiO_2 nanoparticles is greater than that of epoxy resin, an enhancement in strength is produced. This agrees well with the results presented in [31].

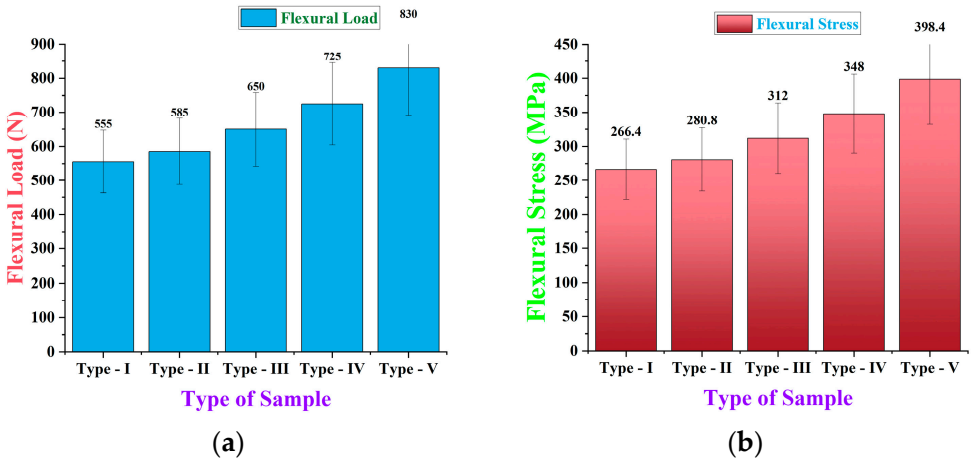


Figure 14. Details of numerical values of (**a**) flexural load and (**b**) flexural stress for 5 different types of samples tested.

Usually, the failure of a composite is affected by one of the following factors. These factors are linked to the type of materials used, their stacking sequence, and their loading direction. When flexural load is applied, the failure of the samples occurs in shear or delamination [30]. In the present study, we observe the occurrence of delamination failure when the sample is subjected to flexural load. Therefore, the fracture happens along the fiber direction. Tension failures are very unlikely during the present flexural tests, as Carbon fibers and Kevlar fibers possess good tensile properties. Moreover, the compressive mode of failure is more likely in the case of flexural tests [32]. Composite failure also depends on the stacking sequence of fibers produced by manufacturing. Usually, when Carbon fibers are placed as the outermost layers on either side of a composite, an increased value of flexural strength can occur, as reported by Ary Subagia and Yonjig Kim [33]. The flexural load applied generates a compressive load at the top end. Hence, this results in a failure called kinking at the center of the load, and if the load is increased, results in fiber pullout. Other potential failures are shearing, micro buckling, and splitting, which were reported by Chensong Dong et al. [31].

Figure 15 shows the sample after the impact test. The impact test is carried out for three samples for each type, and their average values are introduced in Figure 16. The maximum value of impact energy achieved is about 10.1 joules for the Type V sample and a minimum value of 7.7 joules for the Type I sample. The increase in the percentage of the impact energy absorption from Type I to Type V is about 31.2%. Further, when comparing the impact energy of Type V with Type II, the increase is about 20.2 %. Rahmani et al. [34] reported that the impact strength of composites is affected by factors such as the number of laminates and fiber orientation. This effect is identified here because the Type I composites exhibit a very low value of impact energy absorption, whereas Type II samples, which contain a symmetric fiber orientation, show an increased value of impact energy absorption up to 9.09%. Further, the addition of TiO_2 nanoparticles triggers a significant improvement in the values of impact energy absorption. Yet, this variation is almost constant and lesser

with an increase of nearly 0.5 J in each case. The literature also reported that the impact strength of composites may be improved by increasing the number of plies. The number of laminate sheets used in this research is seven, which also contributes to the improvement in the value of impact strength.

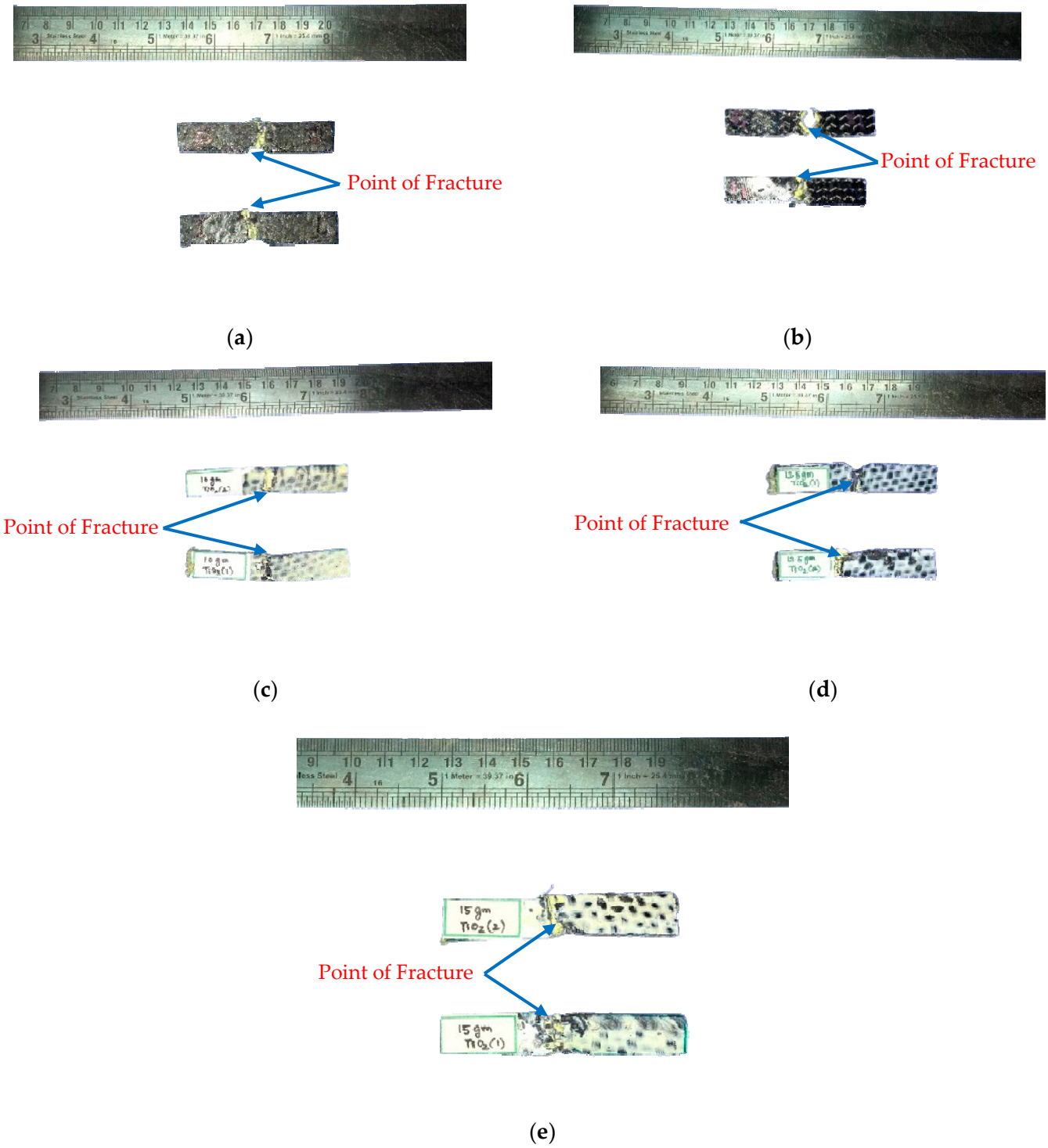


Figure 15. Specimen after impact test for: (**a**) Type I, (**b**) Type II, (**c**) Type III, (**d**) Type IV, and (**e**) Type V.

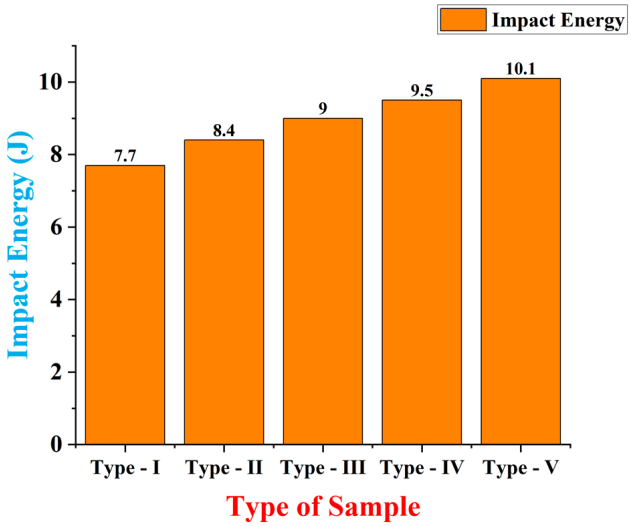


Figure 16. Details of impact test results for 5 different types of samples.

Figure 15 reveals that the failures do not occur exactly on the notch machined in the center. Harris and Bunsell [35] reported that notched areas promote failure, but crack propagation may not follow a straight pathway across the notch itself, rather forming a kinking area near the notch. The fracture that is observed due to TiO_2 nanoparticles' addition (Type III, IV, and V) may be ascribed to a brush type of failure. This results in fibers being pulled out and protruding on both sides of the broken sample. Here, we speculate that Kevlar fibers extend more than that of Carbon fibers. Further, one purpose of adding Carbon fibers is to reduce the length of the fiber pullout length and the probability of resin fragmentation. However, the results show that adding nanoparticles contributes to creating the conventional brush type of failure mode. On the other hand, in the case of Type I and Type II, as reported by Harris and Bunsell [35], the type of failure changes due to the influence of Carbon fibers. In Type I and Type II samples, the brush type failure mode occurs. The failure mode is noted as a reduction in fiber pullout length, corroborating with a pure brittle failure [36].

Figure 17 shows the value of Shore D hardness obtained for different types of samples. The value of hardness is massively improved when the sample has a fiber orientation, as shown with Type II, which shows a much higher value compared to the Type I sample. On the other hand, the improvement in hardness is slightly better for Type III, but not as significant when compared to Type II. Adding 4% (Type IV) and 5% (Type V) TiO_2 nanoparticles produces a significant improvement in hardness. The percentage increase in hardness for Type II compared with Type I is 13.02%. For successive types (i.e., Type III, IV, and V), the percentage increases compared with Type I are 14.8%, 23.5%, and 28.3%, respectively. The increase in hardness in the novel composites is also attributed to better bonding between the matrix and fibers. The addition of nanoparticles corroborates with a uniform distribution of these particles, also contributing to an increase in hardness values.

Figure 18 shows the microstructural investigation for the composite samples studied. Figure 18a reveals that the Carbon–Kevlar hybrid composites are formed by seven layers. In Figure 18b, a magnified view of this sample is presented. There is perfect bonding between the successive layers of the fibers. Figure 18c shows the microstructure generated from the tensile tested sample. Due to the applied tensile load, the fibers are pulled out from their initial location. It is observed that Kevlar fibers are pulled out at a greater length when compared to Carbon fibers. This is because Kevlar fibers yield more than that of Carbon fibers and their strength is lower. The most common type of fracture seen in the composites is brittle fracture. The applied load may also induce delamination and laminate

debonding. This happens when the load exceeds the maximum load capacity of the tested sample. This process (delamination/debonding) may cause ups and downs in the areas of sample failure. Figure 18d shows a magnified view of the same tensile tested sample. There, Carbon fiber bundles are visible together with TiO_2 nanoparticles, which are seen to be attached to the surface of the fibers. The presence of some Carbon fiber and Kevlar fiber debris is also noted on the microstructure. Figure 18e,f show the detail obtained at a higher magnification, in which arrangements of Carbon fiber bundles and Kevlar fiber bundles, respectively, are observed. There, the variation in the length of fibrous bundles is caused by damage associated with the applied load [37].

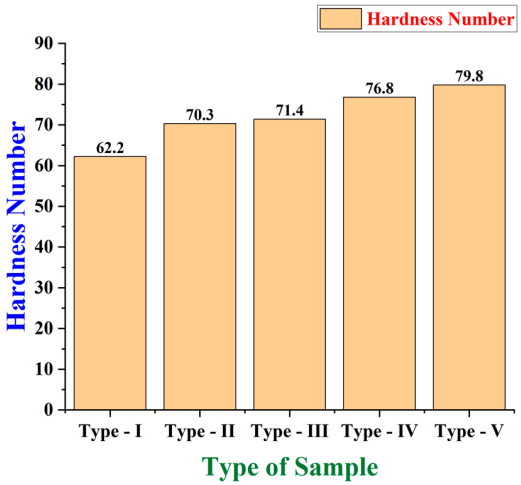


Figure 17. Details of the hardness test results for 5 different types of samples.

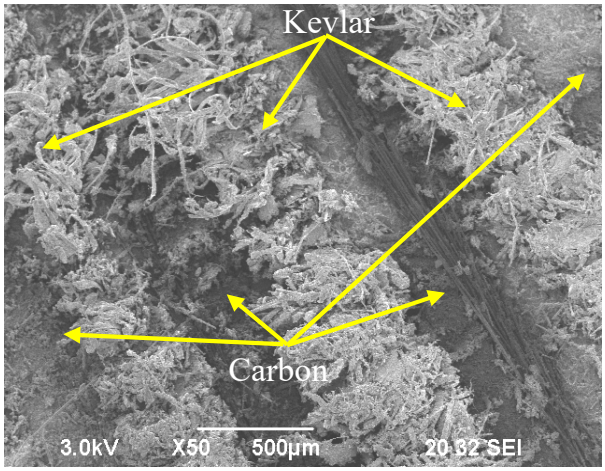
The following Table 4 shows a comparison of the results obtained with other research works.

Table 4. Comparison of results with other research works.

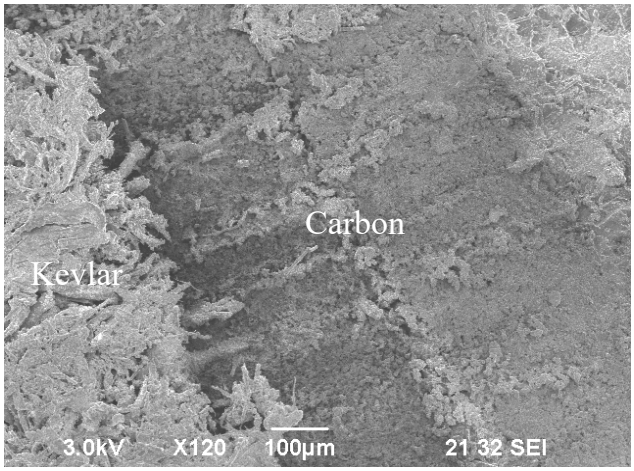
S. No.	Authors	Tensile (MPa)	Flexural (N/mm^2)	Impact (J)	Hardness Shore D
1	Present Work	406	398	10.1	79.8
2	Sulistyo and Wirawan (2024) [38]	181.6	1387	--	--
3	Williams et al. (2011) [39]	314.9	--	--	--
4	Rezza Ruzuqi (2020) [40]	87.054	--	--	--
5	Ajibade et al. (2018) [41]	--	--	--	29.3
6	Jiang et al. (2023) [42]	37	--	63	--
7	Krishnan et al. (2018) [43]	88.70	106.6	92.3 (kJ/m^2)	29.5
8	Salaman, A. J. (2012) [44]	358	--	175 (kJ/m^2)	--

The evaluation of composites manufactured with TiO_2 nano reinforcements shows the distribution of nanoparticles on the composite surface. Figure 18g,h present the microstructure, in which we can see the agglomeration of TiO_2 nanoparticles. This agglomeration may result in a non-uniform strength variation along the surface of the composites. This can be attributed to some manufacturing defects produced during the fabrication of the composites. Generally, whenever the mold is kept inside the die, excess resin comes out of the die due to the pressure applied to the compression molding machine. Further, Figure 18i,j show the surface of the composites with a uniform distribution of TiO_2 nanoparticles. These nanoparticles are stacked on the surface of the fibers and matrix. Therefore, they generate increases in strength, hardness, toughness, and resistance to indentation. Here, the Carbon fiber bundles run parallel to the length of the composites. Some locations present matrix

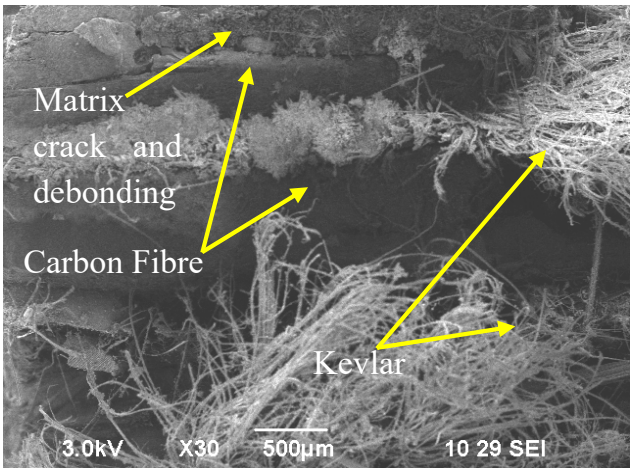
defects, i.e., some pits and valleys that arise due to poor resin distribution. Otherwise, voids may be created due to a poor distribution of resin. Microstructural observation makes it possible to identify the main process caused by mechanical loading, which is beneficial for designing robust and challenging components for the industrial sector [45].



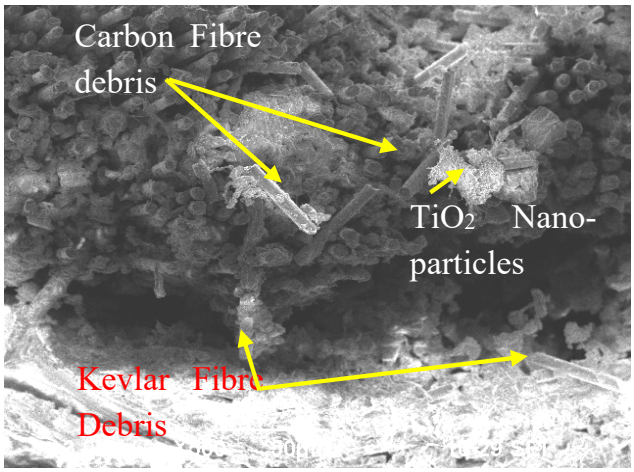
(**a**)



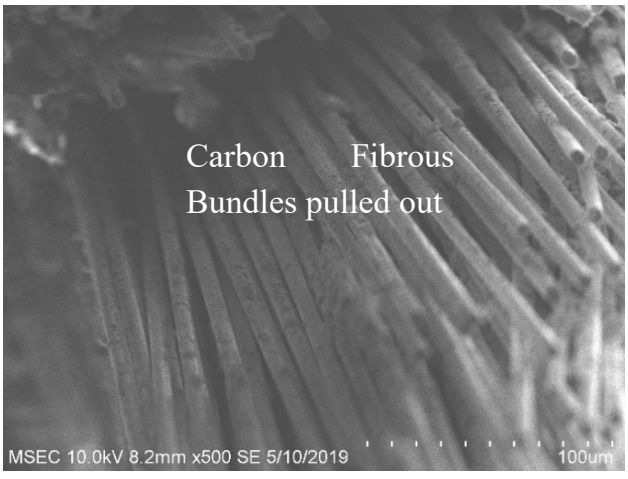
(**b**)



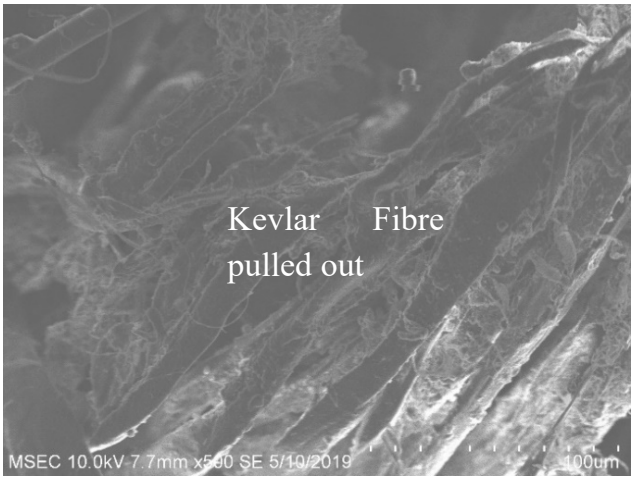
(**c**)



(**d**)



(**e**)



(**f**)

Figure 18. *Cont.*

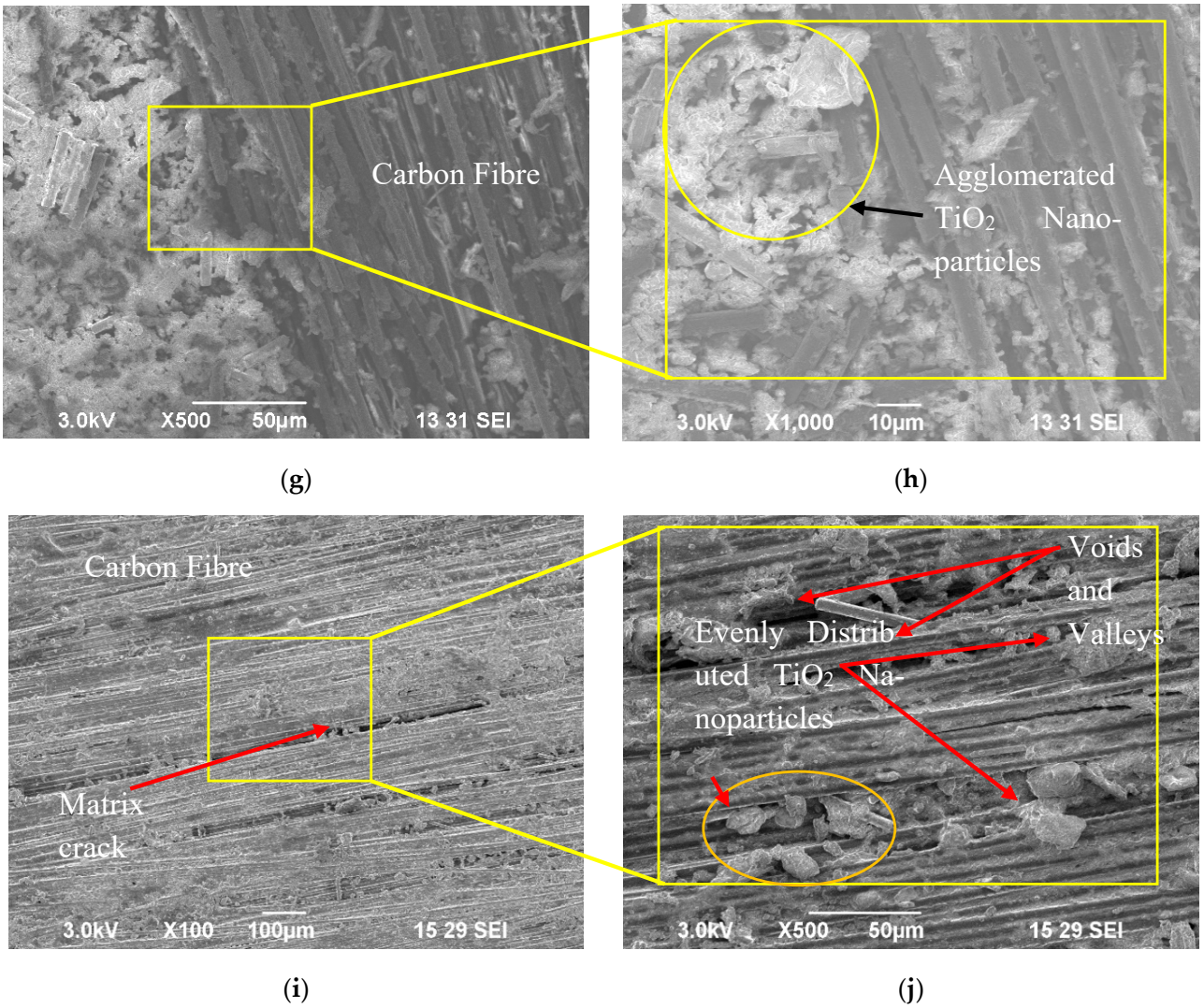


Figure 18. (**a**) Patterns of microstructural morphology of Carbon–Kevlar hybrid composites that contain different layers, (**b**) a magnified view of Carbon–Kevlar hybrid composites, (**c**) microstructure from tensile tested sample, (**d**) magnified view of tensile tested sample, (**e**) Carbon fiber pulled out due to elongation, (**f**) Kevlar fiber pulled out due to elongation, and (**g**–**j**) present microstructure of samples which contain TiO_2 nanoparticles.

4. Conclusions

Five different types of composites were investigated for their performances in terms of mechanical properties, with the following conclusions. The results showed that they are promising candidates for automotive, aerospace, and structural applications.

Symmetric fibers within a specific orientation (Type I) enabled better properties than a random orientation (Type II).

Adding TiO_2 nanoparticles as reinforcements to the matrix permitted further improvement in the composite mechanical performance. A 15% wt TiO_2 nanoparticle addition resulted in a 183.62% increase in tensile strength.

The results of tensile, flexural, impact, and microhardness tests revealed that there was an improvement in the composites' performances not only because of their fiber orientation, but also due to the addition of nanoparticles. The best mechanical properties were achieved with 5 wt% TiO_2 nano reinforcements.

The microstructural investigation allowed us to identify the details of the bonding nature, fiber orientation, and distribution of nanoparticles. It was found that the failure

mechanism of the developed composites was related to fiber damage, pullout, voids, etc. The fracture that was observed due to TiO_2 nanoparticle addition (Type III, IV, and V) was ascribed to the brush type of failure.

Furthermore, application-specific needs should be taken into account when evaluating how cost-effective it is to use these composites in aerospace and automotive applications. This means testing at elevated temperatures and in fire conditions. Such materials can be used to make shapes such as C-section, T-section, and tubular sections. As part of cooperation, we can examine such elements as applications in building structures at the Silesian University of Technology.

Author Contributions: Conceptualization, R.J.H.N. and V.N.J.; methodology, V.N.J. and R.J.; formal analysis, V.N.J. and K.S.; investigation, R.J.H.N.; resources, R.J.H.N.; writing—original draft preparation, R.J.H.N., R.J. and V.N.J.; writing—review and editing, A.N.; supervision, R.J.H.N.; funding, R.J. All authors have read and agreed to the published version of the manuscript.

Funding: This research received no external funding.

Data Availability Statement: The datasets used and analysed during the current study are available from the corresponding author on reasonable request.

Acknowledgments: The corresponding author Rajesh Jesudoss Hynes Navasingh acknowledges the support of Ulam NAWA Postdoctoral Fellowship of Polish National Agency for Academic Exchange programme, Contract Agreement no. BPN/ULM/2022/1/00133/U/00001. The author Krzysztof Stebel acknowledges the support in part by the grant from SUT—subsidy for maintaining and developing the research potential in 2023.

Conflicts of Interest: The authors declare no conflicts of interest.

References

1. Koricho, E.G.; Belingardi, G.; Beyene, A.T. Bending fatigue behavior of twill fabric E-glass/epoxy composite. *Compos. Struct.* **2014**, *111*, 169–178. [CrossRef]
2. Friedrich, K.; Lu, Z.; Hager, A. Recent advances in polymer composites tribology. *Wear* **1995**, *190*, 139–144. [CrossRef]
3. Degrieck, J.; Van Paepegem, W. Fatigue damage modeling of fibre-reinforced composite materials: Review. *Appl. Mech. Rev.* **2001**, *54*, 279–300. [CrossRef]
4. Davim, J.P.; Reis, P. Study of delamination in drilling carbon fibre reinforced plastics (CFRP) using design experiments. *Compos. Struct.* **2003**, *59*, 481–487. [CrossRef]
5. Chand, S. Review carbon fibres for composites. *J. Mater. Sci.* **2000**, *35*, 1303–1313. [CrossRef]
6. Sun, X.; Sun, H.; Li, H.; Peng, H. Developing polymer composite materials: Carbon nanotubes or graphene. *Adv. Mater.* **2013**, *25*, 5153–5176. [CrossRef]
7. Abdullah, S.I.; Ansari, M.N.M. Mechanical properties of graphene oxide (GO)/epoxy composites. *HBRC J.* **2015**, *11*, 151–156. [CrossRef]
8. Pathak, A.K.; Borah, M.; Gupta, A.; Yokozeki, T.; Dhakate, S.R. Improved mechanical properties of carbon fibre/graphene oxide-epoxy hybrid composites. *Compos. Sci. Technol.* **2016**, *135*, 28–38. [CrossRef]
9. Ogasawara, T.; Ishida, Y.; Kasai, T. Mechanical properties of carbon fibre/fullerene-dispersed epoxy composites. *Compos. Sci. Technol.* **2009**, *69*, 2002–2007. [CrossRef]
10. Vaganov, G.; Yudin, V.; Vuorinen, J.; Molchanov, E. Influence of multiwalled carbon nanotubes on the processing behavior of epoxy powder compositions and on the mechanical properties of their fibre reinforced composites. *Polym. Compos.* **2016**, *37*, 2377–2383. [CrossRef]
11. Xu, Y.; Van Hoa, S. Mechanical properties of carbon fibre reinforced epoxy/clay nanocomposites. *Compos. Sci. Technol.* **2008**, *68*, 854–861. [CrossRef]
12. McGrath, L.M.; Parnas, R.S.; King, S.H.; Schroeder, J.L.; Fischer, D.A.; Lenhart, J.L. Investigation of the thermal, mechanical, and fracture properties of aluminaeepoxy composites. *Polymers* **2008**, *49*, 999–1004. [CrossRef]
13. Hynes, N.R.J.; Sankaranarayanan, R.; Tharmaraj, R.; Pruncu, C.I.; Dispinar, D. A Comparative Study of the Mechanical and Tribological Behaviours of Different Aluminium Matrix–Ceramic Composites. *J. Braz. Soc. Mech. Sci. Eng.* **2019**, *41*, 330. [CrossRef]
14. Kardar, P.; Ebrahimi, M.; Bastani, S. Study the effect of nano-alumina particles on physical–mechanical properties of UV cured epoxy acrylate via nano-indentation. *Prog. Org. Coat.* **2008**, *62*, 321–325. [CrossRef]

15. Zhao, H.; Li, R.K.Y. Effect of water absorption on the mechanical and dielectric properties of nano-alumina filled epoxy nanocomposites. *Compos. Part A* **2008**, *39*, 602–611. [CrossRef]
16. Gurunathan, M.K.; Hynes, N.R.J.; Al-Khashman, O.A.; Brykov, M.; Ganesh, N.; Ene, A. Study on the Impact and Water Absorption Performance of Prosopis Juliflora & Glass Fibre Reinforced Epoxy Composite Laminates. *Polymers* **2022**, *14*, 2973. [CrossRef]
17. Zhao, R.; Luo, W. Fracture surface analysis on nano-SiO_2/epoxy composite. *Mater. Sci. Eng. A* **2008**, *483–484*, 313–315. [CrossRef]
18. Mirmohseni, A.; Zavareh, S. Preparation and characterization of an epoxy nanocomposites toughened by a combination of thermoplastic, layered and particulate nano-fillers. *Mater. Des.* **2010**, *31*, 2699–2706. [CrossRef]
19. Chatterjee, A.; Islam, M.S. Fabrication and characterization of TiO_2–epoxy nanocomposites. *Mater. Sci. Eng. A* **2008**, *487*, 574–585. [CrossRef]
20. Zhou, Y.; White, E.; Hosur, M.; Jeelani, S. Effect of particle size and weight fraction on the flexural strength and failure mode of TiO_2 particles reinforced epoxy. *Mater. Lett.* **2010**, *64*, 806–809. [CrossRef]
21. Hamming, M.L.; Qiao, R.; Messersmith, P.; Brinson, L.C. Effects of dispersion and interfacial modification on the macroscale properties of TiO_2 polymer-matrix nanocomposites. *Compos. Sci. Technol.* **2009**, *69*, 1880–1886. [CrossRef] [PubMed]
22. Siddhartha, A.P.; Bhatt, A.D. Functionally graded materials manufacturing techniques: A review. *Mater. Des.* **2011**, *32*, 615–627. [CrossRef]
23. Rajesh, S.; VijayaRamnath, B.; Elanchezhian, C.; Aravind, N.; Rahul, V.V.; Sathish, S. Analysis of Mechanical Behavior of Glass Fibre/Al_2O_3-SiC Reinforced Polymer composites. *Procedia Eng.* **2014**, *97*, 598–606. [CrossRef]
24. Naik, N.K.; Ramasimha, R.; Arya, H.; Prabhu, S.V.; Shamarao, N. Impact response and damage tolerance characteristics of glass-carbon/epoxy hybrid composite plates. *Compos. Part B* **2001**, *32*, 565–574. [CrossRef]
25. *ASTM D638-22*; Standard Test Method for Tensile Properties of Plastics. ASTM International: West Conshohocken, PA, USA, 2022.
26. *ASTM D790-00*; Standard Test Methods for Flexural Properties of Unreinforced and Reinforced Plastics and Electrical Insulating Materials. ASTM International: West Conshohocken, PA, USA, 2000.
27. *ASTM D256-23*; Standard Test Methods for Determining the Izod Pendulum Impact Resistance of Plastics. ASTM International: West Conshohocken, PA, USA, 2023.
28. Hamidon, M.H.; Sultan MT, H.; Ariffin, A.H. Investigation of mechanical testing on hybrid composite materials. In *Failure Analysis in Biocomposites, Fibre-Reinforced Composites and Hybrid Composites*; Woodhead Publishing: Sawston, UK, 2019; pp. 133–156.
29. Lin, G.-M.; Xie, G.-Y.; Sui, G.-X.; Yang, R. Hybrid effect of nanoparticles with carbon fibres on the mechanical and wear properties of polymer composites. *Compos. Part B* **2011**, *43*, 44–49. [CrossRef]
30. Yu, T.; Zhang, Z.; Song, S.; Bai, Y.; Wu, D. Tensile and flexural behaviors of additively manufactured continuous carbon fibre-reinforced polymer composites. *Compos. Struct.* **2019**, *225*, 111147. [CrossRef]
31. Dong, C.; Ranaweera-Jayawardena, H.A.; Davies, I.J. Flexural properties of hybrid composites reinforced by S-2 glass and T700S carbon fibres. *Compos. Part B* **2012**, *43*, 573–581. [CrossRef]
32. Deep, A.; Singh, K.K.; Rawat, P.; Kumar, C.; Behera, R.P. Effect of nano and macro carbon fillers on flexural properties of glass fibre/epoxy composite laminates. *IOP Conf. Ser. Mater. Sci. Eng.* **2018**, *455*, 012007. [CrossRef]
33. Subagia, I.D.G.A.; Kim, Y. A study on flexural properties of carbon-basalt/epoxy hybrid composites. *J. Mech. Sci. Technol.* **2013**, *27*, 987–992. [CrossRef]
34. Rahmani, H.; Najafi SH, M.; Ashori, A. Mechanical performance of epoxy/carbon fibre laminated composites. *J. Reinf. Plast. Compos.* **2014**, *33*, 733–740. [CrossRef]
35. Harris, B.; Bunsell, A.R. Impact properties of glass fibre/carbon fibre hybrid composites. *Composites* **1975**, *6*, 197–201. [CrossRef]
36. Hynes, N.R.J.; Vignesh, N.J.; Barile, C.; Velu, P.S.; Ali, M.A.; Raza, M.H.; Pruncu, C.I. Mechanical and microstructural characterization of hybrid fiber metal laminates obtained through sustainable manufacturing. *Arch. Civ. Mech. Eng.* **2022**, *22*, 35. [CrossRef]
37. Hynes, N.R.J.; Vignesh, N.; Jappes, J.W.; Velu, P.S.; Barile, C.; Ali, M.A.; Farooq, M.U.; Pruncu, C.I. Effect of stacking sequence of fibre metal laminates with carbon fibre reinforced composites on mechanical attributes: Numerical simulations and experimental validation. *Compos. Sci. Technol.* **2022**, *221*, 109303. [CrossRef]
38. Sulistyo, A.B.; Wirawan, W.A. Evaluation of tensile strength and flexural strength of GFRP composites in different types of matrix polymers. *J. Achiev. Mater. Manuf. Eng.* **2024**, *123*, 49–57. [CrossRef]
39. Williams, T.; Hosur, M.; Theodore, M.; Netravali, A.; Rangari, V.; Jeelani, S. Time Effects on Morphology and Bonding Ability in Mercerized Natural Fibers for Composite Reinforcement. *Int. J. Polym. Sci.* **2011**, *2011*, 192865. [CrossRef]
40. Ruzuqi, R. Tensile Strength Analysis of Polymer Composite Materials Fiber Reinforced in the Fiber boat Application. *J. Res. Opin.* **2020**, *7*, 2763–2769. [CrossRef]
41. Ajibade, O.A.; Agunsoye, J.O.; Oke, S.A. Experimental investigation of micro-hardness behaviour of dual blended reinforced polymer matrix composites of five selected fortifiers. *Eur. J. Mater. Sci. Eng.* **2018**, *3*, 68–92. Available online: https://ir.unilag.edu.ng/handle/123456789/7681 (accessed on 11 July 2023).

42. Jiang, L.; Zhou, Y.; Jin, F.; Hou, Z. Influence of Polymer Matrices on the Tensile and Impact Properties of Long Fiber-Reinforced Thermoplastic Composites. *Polymers* **2023**, *15*, 408. [CrossRef] [PubMed]
43. Krishnan, T.; Jayabal, S.; Krishna, V.N. Tensile, flexural, impact, and hardness properties of alkaline-treated Sunnhemp fiber reinforced polyester composites. *J. Nat. Fibers* **2020**, *17*, 326–336. [CrossRef]
44. Salaman, A.J. Tensile and impact properties of polystyrene matrix composites reinforced by palm natural fibers and carbon fibers. *Acad. Res. Int.* **2012**, *3*, 114.
45. Desnica, E.; Đurđev, M.; Vaščić, B.; Turmanidze, R.; Dašić, P. Determination of a Safety Factor of a Car Wheel Rim Using Finite Element Analysis in SolidWorks. *Appl. Eng. Lett.* **2022**, *7*, 163–171. [CrossRef]

Disclaimer/Publisher's Note: The statements, opinions and data contained in all publications are solely those of the individual author(s) and contributor(s) and not of MDPI and/or the editor(s). MDPI and/or the editor(s) disclaim responsibility for any injury to people or property resulting from any ideas, methods, instructions or products referred to in the content.